EFFECTS OF PROCESS PARAMETERS ON MICROARC OXIDATION FILM LAYERS OF POROUS TITANIUM

FAN, X. P.

Panzhihua University, Panzhihua, Sichuan, PR China
e-mail: fanxingping123@163.com

(Received 8th Mar 2019; accepted 21st May 2019)

Abstract. In order to better understand the specific effect of process parameters on porous titanium micro-arc oxidation coating. In this paper, TiO_2 membrane layer was prepared on porous titanium matrix with 67 % porosity by microarc oxidation method (MAO), which use a phosphoric acid solution as electrolyte. The samples were characterized using XRD and SEM. The results showed that the samples prepared under the experimental parameters of 350 V and 30 min had a good surface morphology and could provide a higher specific surface area. After soaking in SBF for 7 days, the formation of hydroxyapatite (HA) can be induced, indicating that porous titanium after micro-arc oxidation modification has good biological activity.
Keywords: *phosphoric acid, hydroxyapatite, carbon dioxide film, process parameters, biological activity*

Introduction

Titanium (Ti) and its alloys are widely used as hard tissue repair materials in clinics owing to their high biocompatibility (Choi and Kim, 2016; Nune et al., 2016; Thanh and Do, 2018). However, their far larger elastic moduli and the mismatched mechanical properties compared to human bones would lead to post-implant stress shield and finally to the loosening and failure of implants (Nomura et al., 2005; Shrestha and Baral, 2018). Nevertheless, the emerging porous structures can efficiently improve the mechanical properties of Ti to the levels of human bone tissues. Moreover, porous Ti has high biocompatibility, and (Hao, 2018) its unique structures are favorable for the body fluid transmission and tissue regeneration / reconstruction and accelerate the healing process. (Zhang et al., 2017). Generally, a higher porosity offers a larger space for tissue growth, which is favorable for the inward growth of peripheral cells and the growth of new bones and strengthens the bio-fixation with bone tissues (Wen et al., 2001; Ali et al., 2018).

However, Ti is a biologically inert material that can hardly bind with bone tissues to form bone bonding (Wang et al., 2014; Rahim et al., 2018), which limits its further application in the medical field (Das et al., 2016; Qiao, 2018). Thus, surface modification is required to improve the biological performances of porous Ti. The emerging microarc oxidation surface modification in recent years can be used to prepare porous ceramic coating layers on surfaces of Ti and thereby to largely improve its properties (Chien et al., 2017; Gautam et al., 2019). The phases and morphology largely affect the bioactivity of porous ceramic films (Zhao et al., 2014), but there is rare research on microarc oxidation coating of porous Ti. Thus, the microarc oxidation technology was used to prepare porous coatings on the porous Ti matrix. The effects of anode voltage and oxidation time on the surface morphology and phases of the coatings were systematically studied (Chen et al., 2017; Dali and Kamarudin, 2018). The findings offer some reference for subsequent research.

http://www.aloki.hu ● ISSN 1589 1623 (Print) ● ISSN 1785 0037 (Online)
DOI: http://dx.doi.org/10.15666/aeer/1704_86318641

Materials and Method

Preparation of porous Ti

The 300-mesh commercial pure Ti powder and NH_4HCO_3 (granularity=100-300 μm) as the pore-forming agent were mixed at the mass fraction ratio of 1:1, uniformly stirred, and placed (Zhang et al., 2018; Masri and Samsudin, 2018) into a mold, which was pressed by a miniature hydraulic press at the pressure of 80 MPa. The molded specimens were preserved in an ordinary muffle furnace at 100ºC for 5 h in order to completely remove the pore-forming agent, then heated to 1300ºC in a vacuum sintering furnace (< 10^{-3} MPa), heat-preserved for 2 h and naturally cooled, forming the porous Ti substrate.

Preparation of surface TiO_2 films on porous Ti via microarc oxidation

The sintered porous Ti was cut into sheets (Φ10 mm × H2 mm), which were ultrasonically washed with ethanol and deionized water and then dried. (Zhang et al., 2018). The porous Ti sheets were used as the anode, graphite sheets as the cathode, and a 0.5 mol/L H_3PO_4 solution as the electrolytic solution in the microarc oxidation experiments at the time of 5 - 30 min and voltage of 250-450 V. When the electrolytic solution was controlled below 30ºC, porous Ti MAO films were formed and the oxidized specimens were washed in distilled water and dried.

Characterization of TiO_2 films

Morphology was observed under a Quanta200 scanning electron microscope (SEM) and phases were analyzed under an X'Pert Pro MPD X-ray diffractometer (XRD).

Bioactivity experiments

A simulated body fluid (SBF) was made according to the composition by Tadashi Kokubo. The specimens after the above microarc oxidation were soaked in the SBF at 37ºC. The SBF was changed once every day. After 7 days, the specimens were taken out, rinsed with deionized water and air-dried.

Results and discussion

Effects of electrode voltage

Effects on the surface morphology of microarc oxidized film layers

The figure below (*Fig. 1*) shows the surface morphology of the oxidized films prepared after 30 min of oxidation at different electrode voltages. Clearly, (Kang et al., 2017) numerous fine micropores (1-2 μm) were formed on surfaces at the constant voltage of 250 V (*Fig. 1a*). At the voltage of 300 V, however, the specimen surfaces were uneven, with irregularly-shaped heaves in some places and irregular porous surfaces in other places, and the micropores were minor, unevenly-sized and nonuniformly distributed *(Fig. 1b*). At the voltage of 350 V, the surface oxidation films were rough, and the number of micropores significantly increased, but the sizes and distributions were uniform, and the pore sizes were enlarged to 4 - 6 μm (*Fig. 1c*). At the voltage of 450 V, the micropores on their surface oxidation films were significantly enlarged, but the numbers considerably decreased, and a part of the micropores fused

http://www.aloki.hu ● ISSN 1589 1623 (Print) ● ISSN 1785 0037 (Online)
DOI: http://dx.doi.org/10.15666/aeer/1704_86318641

and the walls were broken *(Fig. 1d*). The above results suggest that the pores in the surface films are gradually enlarged and the numbers decline along with the increase of electrode voltage.

This was because due to the overly low voltage, the resulting oxidation films were very thin and weak and could be easily punctured, (Kai et al., 2018; Babaranti et al., 2019) and together with the low discharge quantity, the resulting micropores were large in number and small in size. At high voltage, the enlarged discharge channels due to intense discharge led to the enlarged pores. Thus, when constant-voltage 250 V was applied, the low voltage, small discharge and gentle surface reactions made it easier to puncture the surface thin films, and consequently, a large number of small-sized micropores were formed. At voltage 300 V (Yang et al., 2019), the relatively low voltage and small discharge decelerated the metal surface oxidation, and thus decreased the numbers of micropores on the oxidation films. The slow oxidation led to less heat release and nonuniform oxidation, and irregular convexes and irregular micropores were formed on the oxidation film layers. As the electrode voltage rose to 350 V, the voltage and discharge increased and the metal surface oxidation was quickened, (Zeng et al., 2018) which led to the increased amount of uniformly-distributed micropores on the oxidation films. At the voltage of 450 V, the excessive voltage led to intense discharge, while the released high-energy caused micropore melting and enlarged the discharge channels and micropores.

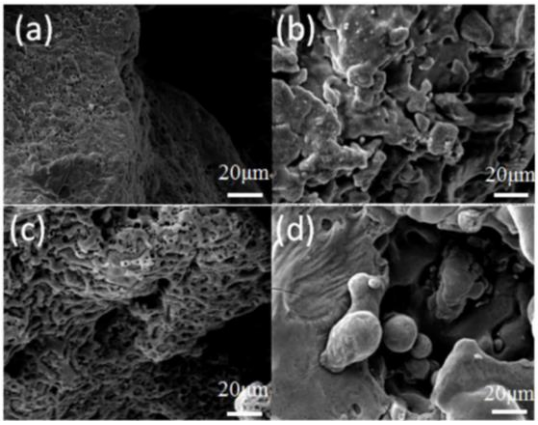

Figure 1. *Surface morphology of specimen under different voltage treatment (a) 250V; (b) 300V; (c) 350V; (d) 450V*

Moreover, (Sheng et al., 2018) the film thickening or densening reduced the conductivity, thereby decelerated the metal surface oxidation and decreased the amount of micropores on the oxidation film layers (Zhu et al., 2008; Pazand and Hezarkhani, 2018). At the electrode voltage of 450 V, evident cracks appeared at the oxidation film surfaces and between pores (*Fig. 1d*). The possible reason was that at higher voltage, the discharge quantity increased and the melting led to the formation of more oxides, (Tang et al., 2019) but during the sudden cooling under the action of external electrolytic solutions, the melts gradually clustered together rather than slowly dispersing or solidifying, leading to the formation of internal stress inside the structures. As the microarc oxidation proceeded, (Xiao, 2019) the inner stress was gradually intensified and finally was macroscopically embodied as local forced cracking on the oxidation films, which explained the formation of microcracks.

http://www.aloki.hu ● ISSN 1589 1623 (Print) ● ISSN 1785 0037 (Online)
DOI: http://dx.doi.org/10.15666/aeer/1704_86318641

According to the basic principles of microarc oxidation, as the microarc oxidation reaction proceeds, the electrode voltage, after exceeding the critical level, will puncture the relatively weak parts on the surfaces of the anode specimens. At the early stage of microarc oxidation, the newly- formed oxide layer is very weak and is likely to be first penetrated, and the short-term overly high temperature subjects the locally-discharged anode to splashed melting, forming current channels for discharge, and after a certain period of external cooling, the penetrated oxidation film layer and the current channels are all reserved. At the same place of puncturing, the new matrix is oxidized into a new oxidation film layer, and the weak parts are punctured again. Thereby, this procedure circulates and consequently the oxidation film layer accumulates and thickens, forming a porous film structure on specimen surfaces in which large pores cover small pores (*Fig. 1c*). In this structure, the film layers and the matrix are mutually inlayed and bond more firmly, which also enlarge the specific surface areas. After 30 min of oxidation, when the constant voltage is 350 V, porous microarc oxidation films with rough surfaces and more micropores are formed on specimen surfaces, and the large pores in the micropores cover the small pores. Under this condition, the specific surface areas are the largest, and the oxidation film layers bond firmly with the matrix. It is deduced that microarc oxidation for surface processing of porous Ti would form the most ideal microarc oxidation films under this condition.

Effects of electrode voltage on the phases of the microarc oxidation films

The following figure shows the XRD images of the surface oxidation films formed from microarc oxidation at different electrode voltages. Clearly, the diffraction peaks of Anatase TiO_2 are very obvious (*Fig. 2*), suggesting the surface oxidation films formed from microarc oxidation under different conditions are all rich in Anatase TiO_2, (Selvaraj, 2017) which is the major component of the oxidation film layers.

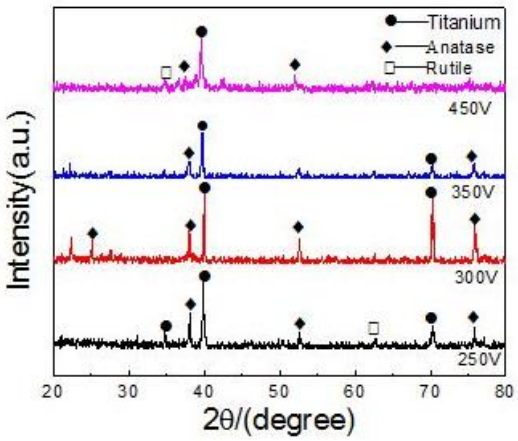

Figure 2. *X-ray diffraction (XRD) patterns of microarc oxide film with different electrode voltage*

Moreover, the diffraction peaks of the base material -- pure Ti are also very strong, but the peaks of Rutile TiO_2 are very weak and only appear at a part of the electrode voltages. These XRD results imply the major phase of the oxidation films formed under different oxidation conditions is anatase TiO_2, and Rutile TiO_2 did appear under certain

http://www.aloki.hu ● ISSN 1589 1623 (Print) ● ISSN 1785 0037 (Online)
DOI: http://dx.doi.org/10.15666/aeer/1704_86318641

conditions, but no rules concerning its concentration were found. This is because rutile TiO_2 has higher activation energy than anatase TiO_2, and the conversion from anatase TiO_2 to rutile TiO_2 relies on very high temperature. Thus, the reason why the rutile TiO_2 concentration did not increase with the rising electrode voltage was deduced. Specifically, the temperature during the microarc oxidation was controlled by the cooling in an ice-water mixture, which was hard to reach the high-temperature needed for the formation of rutile TiO_2. As a result, in the surface oxidation film layers after the microarc oxidation under different conditions, the rutile TiO_2 concentration did not change regularly and was very low.

Effects of time

Effects of time on surface morphology of microarc oxidized films

The figure below shows the surface morphology (×500) of the oxidation films prepared under electrode voltage of 350 V and different time durations (*Fig. 3*). Compared with the blank group (*Fig. 3a*), when the microarc oxidation proceeded under the constant voltage of 350 V, surface porous film layers were formed and the surface roughness was significantly intensified with the reaction time prolonged from 5 to 30 min. At this magnification factor, the specimen surfaces after 5 min of oxidation became rough and contained numerous fine micropores (*Fig. 3*). The surface roughness decreased after 15 to 30 min of oxidation. After 30 min of oxidation, porous film layers containing numerous evenly-distributed and large-sized pores were evidently formed (*Fig. 3d*). Clearly, the numbers and sizes of micropores in the film layers both changed at the same electrode voltage and after different durations of oxidation.

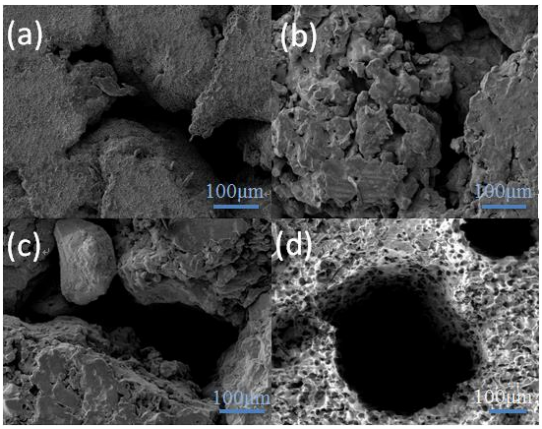

Figure 3. *Low ploid morphology (500 ×) of microarc oxide film surface at different oxidation times*
(a) 5 min; (b) 15min; (c) 25 min; (d) 30 min

The figure below shows the surface morphology (×3000) of the oxidation films prepared under the same electrode voltage of 350 V and different time durations (*Fig. 4*). During the microarc oxidation at the constant voltage of 350 V, very rough porous oxidation film layers were formed after 5 min of oxidation, which contained numerous micropores below 5 μm and were obviously melted (*Fig. 4a*). After 15 min of oxidation, the surface roughness decreased significantly and the numbers of micropores decreased, and the porous film layers contained size-varying and unevenly-distributed

http://www.aloki.hu ● ISSN 1589 1623 (Print) ● ISSN 1785 0037 (Online)
DOI: http://dx.doi.org/10.15666/aeer/1704_86318641

micropores, and the pore sizes decreased, the small pores were in size of ~ 500 nm and the large pores were about 3 μm (*Fig. 4b*). After 25 min of oxidation, the surface oxidation film layers were relatively even, and the sizes (1-2 μm) and distribution of micropores were relatively uniform (*Fig. 4c*). After 30 min, the surface oxidation films were very regular and formed a complete porous structure of small pores in large pores, but the micropores significantly decreased in number and considerably enlarged to about 6 μm (*Fig. 4d*). Clearly, with the prolonging of time before 25 min, the surface roughness gradually decreased, and the micropore distribution in the oxidation film layers became uniform, but the pore sizes decreased slowly. At about 30 min, the micropores were significantly enlarged in size and obviously decreased in numbers, and the porous layer structure of small pores in large pores was the most regular. Thus, at a constant voltage of 350 V was applied, the porous oxidation film layers formed from the micro-arc oxidation were optimized when the oxidation time was 30 min.

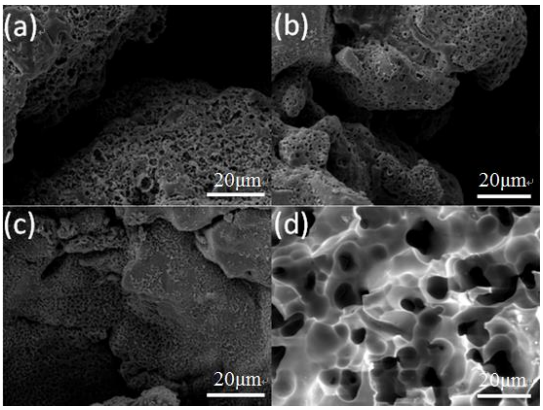

Figure 4. *The surface of the micro-arc oxide film has a high multiple morphology(3000 ×) (a) 5 min at different oxidation times; (b) 15min; (c) 25 min; (d) 30 min*

According to the fundamental principles of oxidation, at the early stage of reaction after 5 min of oxidation, a weak oxidation film layer that could be easily punctured was first formed on the surfaces of the base material. At the voltage of 350 V, the discharge and energy were very large, but the corresponding discharge channels were very small, and numerous fine-sized micropores were formed. However, the instant high-energy release would melt the walls of a part of the surface fine micropores, locally forming large-sized micropores (*Fig. 4a*). With the oxidation time prolonged from 15 to 25 min, the oxidation film layers thickened, reducing conductivity and making the films unpuncturable, but the residual discharge channels were gradually narrowed. The micropores formed at this moment decreased in size, while the residual energy accumulated inside the porous layer structures and would not easily released, leading to the gradual decrease of surface roughness (*Fig. 4b,c*). After 30 min of oxidation, due to the small discharge channels and the gradual energy accumulation, the relatively high energy caused the ablation of film layers and the consequent local melting of micropore walls, forming a smaller amount of larger-sized micropores. At this moment, the oxidation, dissolution and solidification speeds were relatively balanced and thus, regular porous layer surfaces with large pores containing small pores were formed (*Fig. 4a*). It was deduced that as the oxidation time was prolonged, surface ablation would be intensified and thereby more micropores were melted, and consequently, the

http://www.aloki.hu ● ISSN 1589 1623 (Print) ● ISSN 1785 0037 (Online)
DOI: http://dx.doi.org/10.15666/aeer/1704_86318641

oxidation film layers might be punctured and locally shed (Yan et al., 2010). Thus, the time of microarc oxidation should be controlled within a reasonable range.

Effects of time on the phases of the microarc oxidation film layers

The figure below (*Fig. 5*) shows the XRD images of the surface oxidation films formed from different time durations of microarc oxidation. Clearly, the diffraction peaks of Anatase TiO2 are very obvious (*Fig. 5*), suggesting the surface oxidation films formed from different time durations of microarc oxidation are all rich in anatase TiO_2, which is the major phase of the oxidation film layers.

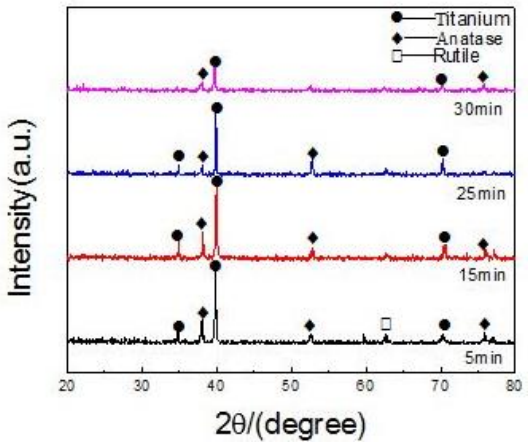

Figure 5. *XRD patterns of microarc oxide films at different oxidation times*

Effects of modification on bioactivity

The figure below (*Fig. 6*) shows the morphology of porous Ti (30 min of oxidation at 350 V, or without oxidation) after soaking in SBF for 7 days. After the non-oxidized porous Ti was soaked in the SBF, new substances were formed (*Fig. 6a*), but in the oxidized porous Ti, the surfaces were fully covered by a sediment after 7 days of mineralization (*Fig. 6b*). XRD patterns confirm this sediment is apatite (*Fig. 7*).

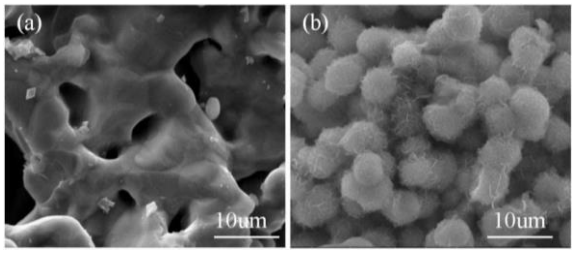

Figure 6. *Morphology of biomimetic mineralization of SEM(a) and(b) before and after microarc oxidation after 7 days of soaking in SBF with porous titanium oxidized by 350V voltage, respectively*

Microarc oxidation, also called plasma electrolysis oxidation or anode sparkle oxidation, is a relatively convenient technique to prepare oxide layers on metal surfaces. Compared with common anode oxidation, its major difference is the higher oxidation

http://www.aloki.hu ● ISSN 1589 1623 (Print) ● ISSN 1785 0037 (Online)
DOI: http://dx.doi.org/10.15666/aeer/1704_86318641

voltage. After microarc oxidation, surface coatings can form on porous metals or irregularly-shaped metals that have complex geometric morphology. The principle of this method in activating Ti and its alloys is attributed to the effect of microstructures on biological reactions. Chen et al. (2010) created different crystal forms of TiO_2 coatings atop β Ti alloys by regulating the microarc oxidation voltage and investigated the effects of crystal forms on osteoblast growth.

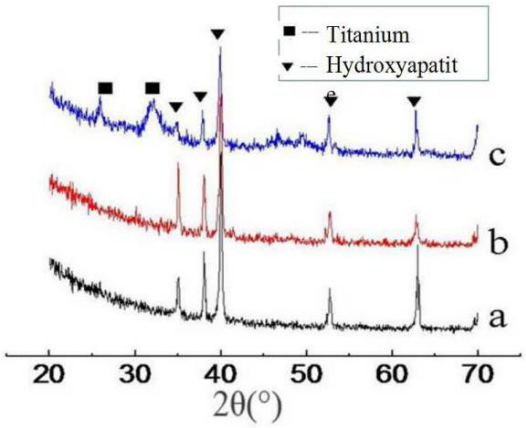

Figure 7. *XRD map of different samples*
a) Porous titanium prepared by vacuum sintering; b) is a sample of porous titanium that has not been treated with microarc oxidation after being soaked in SBF for 7 days; c) is a porous titanium after microarc oxidation (voltage 350V, oxidation time 30 min) and then soaked in SBF for 7 days

They found the TiO_2 after microarc oxidation possessed the bioactivity and Ca deposition ability like cells. Bayati et al. (2010) found with the increasing oxidation voltage, the surface pore sizes and roughness both significantly increased, but the number of pores first rose and then declined, while the contact angle first decreased and then enlarged. Furthermore, the variation of hydrophilicity was caused by mainly two factors, including the existence of surface oxidation films and the variation of specific surface (Yang et al., 2019). Since we conducted microarc oxidation on surfaces of porous Ti, the oxidation parameters were different from those of dense Ti. Firstly, the films formed under our experimental conditions were all porous and were TiO_2 films, and these film microstructures were favorable for the formation of the precipitate HA. Secondly, the hierarchical microstructures formed from porous Ti oxidation increased the specific surface areas and hydrophilicity. The enlarged specific surface areas enhanced the specific surface energy and surface activity of porous Ti, which created more sites for apatite nucleation. The more hydrophilic surfaces were more likely to contact and bind with polar ions in SBF, which accelerated the apatite nucleation and crystallization. The different mineralization results in our study can be explained from two reasons. The first reason is the change of surface morphology, since the increase in pore number and specific surface area offer more sites for the nucleation of precipitates. The second reason might be related to the phases of post-oxidation surface film layers. The above analysis suggests the surface activity can be enhanced by surface-modifying the porous Ti through microarc oxidation. Thus, microarc oxidation may be used to modify the surface activation of porous Ti.

http://www.aloki.hu ● ISSN 1589 1623 (Print) ● ISSN 1785 0037 (Online)
DOI: http://dx.doi.org/10.15666/aeer/1704_86318641

Conclusions

(1) When the time of oxidation was constant, the pores in the surface oxidation film layers gradually increased in size and decreased in number with the increment of electrode voltage. The oxidized film layers contained both rutile TiO_2 and anatase TiO_2.

(2) When the voltage was constant, with the prolonging of oxidation time within 5 and 25 min, the surface roughness gradually decreased, the micropores on the oxidation film layers became uniformly-distributed and decreased slowly in size. At about 30 min, the micropores were significantly enlarged in size and obviously decreased in number, and the porous layer structure of small pores in large pores was the most regular. The oxidation film layers were mainly composed of anatase TiO_2.

(3) After 30 min of oxidation at voltage 350 V, the oxidized film layers on pore walls of porous Ti became uniform micropore structures in pore size of ~ 6 μm, and these structures had large specific surface areas, which were the optimal experimental parameters under the tested conditions.

(4) The porous Ti modified by microarc oxidation induced apatite generation and was more bioactive compared with the porous Ti surface without microarc oxidation.

In the future, when the porous Ti micro-arc oxidation film is applied in specific fields, all the parameters in this paper can provide beneficial value.

Aknowledgements. This study was funded by Panzhihua University Doctor Foundation (0210600011).

REFERENCES

[1] Ali, W., Nasir, M. S., Nasir, A., Rashid, H., Ayub, I., Gillani, S. H., Latif, M. J. (2018): Assessment Of Carbon Footprints In Terms Of Co2 Of Diesel Generator, Pakistan. – Earth Sciences Pakistan 2(1): 15-17.

[2] Babaranti, O., Horn, S., Jowett, T., Frew, R. (2019): Isotopic signatures in Mytilus galloprovincialis and Ulva latuca as bioindicators for assessing discharged sewage effluent in coastal waters along Otago Peninsula, New Zealand. – Geology, Ecology, and Landscapes 3(1): 53-64.

[3] Bayati, M. R., Molaei, R., Kajbafvala, A., Zanganeh, S., Zargar, H. R., Janghorban, K. (2010): Ivestigation on hydrophilicity of micro-arc oxidized TiO_2 nano/micro-porous layers. – Electrochim acta 55: 5786-92.

[4] Chen, H. T., Chung, C. J., Yang, T. C., Chiang, I. P., Tang, C. H., Chen, K. C., He, J. L. (2010): Osteoblast growth behavior on micro-arc oxidizedβ-titanium alloy. – Surf coat tech 205: 1624-9.

[5] Chen, L., Tang, M., Chen, C., Chen, M., Luo, K., Xu, J., Zhou, D., Wu, F. (2017): Efficient bacterial inactivation by transition metal catalyzed auto-oxidation of sulfite. – Environmental Science & Technology 51(21): 12663-12671.

[6] Chien, C. S., Hung, Y. C., Hong, T. F., Wu, C. C., Kuo, T. Y., Lee, T. M., Liao, T. Y., Lin, H. C., Chuang, C. H. (2017): Preparation and characterization of porous bioceramic layers on pure titanium surfaces obtained by micro-arc oxidation process. – Applied Physics A: Materials Science and Processing 123(3): 204-303.

[7] Choi, J. W., Kim, N. (2015): Clinical application of three-dimensional printing technology in craniofacial plastic surgery. – Archives of Plastic Surgery 42(3): 267-277.

[8] Dali, N. M., Kamarudin, K. S. N. (2018): The Effect of Cosurfactant In Co2 Absorption In Water – In – Oil Emulsion. – Environment & Ecosystem Science 2(2): 42-46.

http://www.aloki.hu ● ISSN 1589 1623 (Print) ● ISSN 1785 0037 (Online)
DOI: http://dx.doi.org/10.15666/aeer/1704_86318641

[9] Das, I., Chattopadhyay, S., Mahato, A., Kundu, B., De, G. (2016): Fabrication of a cubic zirconia nanocoating on a titanium dental implant with excellent adhension, hardness and biocompatibility. – RSC Advances 6(64): 59030-59038.
[10] Gautam, A., Batra, R., Singh, N. (2019): A Study On Use Of Rice Husk Ash In Concrete. – Engineering Heritage Journal 1(1): 01-04.
[11] Hao, M. (2018): Numerical Simulation of Borehole Acoustic Field of Adhering Sand Casing Well. – Acta Microscopica 27(4): 305-308.
[12] Kai, W., Shengzhe, Z., Yanting, Z., Jun, R., Liwei, L., Yong, L. (2018): Synthesis of porous carbon by activation method and its electrochemical performance. – Int. J. Electrochem. Sci 13(11): 10766-10773.
[13] Kang, L., Zhang, Y. J., Zhang, L., Zhang, K. (2017): Preparation, characterization and photocatalytic activity of novel CeO2 loaded porous alkali-activated steel slag-based binding material. – International Journal of Hydrogen Energy 42(27): 17341-17349.
[14] Masri, E., Samsudin, M. D. M. (2018): Optimization Performance Of Biological Cathodic Protection System Using Organic Waste. – Environment & Ecosystem Science 2(2): 25-29.
[15] Nomura, N., Kohama, T., Oh, I. H., Hanada, S., Chiba, A., Kanehira, M., Sasaki, K. (2005): Mechanical properties of porous Ti-15-Mo-3Al compacts prepared by powder sintering. – Materials Science & Engineering C 25: 330-335.
[16] Nune, K. C., Kumar, A., Murr, L. E., Misra, R. D. (2016): Interplay between self-assembled structure of bone morphogenetic protein-2 (BMP-2) and osteoblast functions in three-dimensional titanium alloy scaffolds: stimulation of osteogenic activity. – Journal of Biomedical Materials Research Part A 104(2): 517-532.
[17] Pazand, K., Hezarkhani, A. (2018): Predictive Cu porphyry potential mapping using fuzzy modelling in Ahar–Arasbaran zone, Iran. – Geology, Ecology, and Landscapes 2(4): 229-239.
[18] Qiao, F. (2018): The Study On The Integration Of Green Architecture And Appropriate Technology. – Engineering Heritage Journal 2(2): 01-03.
[19] Rahim, Y., Khan, M. S., Mughal, S. (2018): Petrography Of Sandstone Of The Lumshiwal Formation From Eastern Hazara, Khyber Pakhtunkhwa, Pakistan: Implications For Provenance, Diagenesis And Environments Of Deposition. – Earth Sciences Pakistan 2(2): 01-06.
[20] Selvaraj, P. (2017): Segregation of Degradable and Non Degradable using Sensor. – Revista de la Facultad de Agronomia de la Universidad del Zulia 34(3): 306-312.
[21] Sheng, J., Su, J., La, P., Ren, J., Ma, J., Shi, Y., Song, Y. (2018): Progress of In-Situ Study on Mechanical Properties for Micro/Nano-Structured Alloy. – Journal of Nanoelectronics and Optoelectronics 13(5): 637-645.
[22] Shrestha, A., Baral, S. (2018): Socioeconomic Factors Affecting Awareness And Adaption Of Climate Change: A Case Study Of Banke District Nepal. – Earth Sciences Malaysia 2(2): 20-24.
[23] Tang, Y., Li, L., Wang, C., Chen, M., Feng, W., Zou, X., Huang, K. (2019): Real-time detection of surface deformation and strain in recycled aggregate concrete-filled steel tubular columns via four-ocular vision. – Robotics and Computer-Integrated Manufacturing 59: 36-46.
[24] Thanh, L. D., Do, P. V. (2018): Streaming Current Induced By Fluid Flow In Porous Media. – Earth Sciences Malaysia 2(1): 22-28.
[25] Wang, F. H., Zhang, S. S., Shu, J. Y., Gao, Y. (2014): Effects of surface modifacation titanium implants on the osseointegration. – Chinese Journal of Tissue Engineering Research 18(52): 8491-8497.
[26] Wen, C. E., Mabuchi, M., Yamada, Y., Shimojima, K., Chino, Y., Asahina, T. (2001): Processing of biocompatible porous Ti and Mg. – Sctipta Materialia 45(10): 1147-1153.
[27] Xiao, F. (2019): Multi-sensor data fusion based on the belief divergence measure of evidences and the belief entropy. – Information Fusion 46: 23-32.

http://www.aloki.hu ● ISSN 1589 1623 (Print) ● ISSN 1785 0037 (Online)
DOI: http://dx.doi.org/10.15666/aeer/1704_86318641

[28] Yan, F. Y., Shi, Y. L., Mo, W. Y. (2010): Influence of oxidation time on micro-arc oxidation coating on titanium substrate. – Surface technology 39(4): 42-44.
[29] Yang, Y. X., Li, H., Zheng, W. K., Yun, B., Liu, Z. M., Zhang, J. J. (2019): Experimental Study on Calcining Process of Secondary Coated Ceramsite Solidified Chromium Contaminated Soil. – Science of Advanced Materials 11(2): 208-214.
[30] Zeng, L., Guo, X. P, Zhang, G. A., Chen, H. X. (2018): Semiconductivities of passive films formed on stainless steel bend under erosion-corrosion conditions. – Corrosion Science 144: 258-265.
[31] Zhang, Y. Y., Li, Y. A., Bai, C. G. (2017): Microstructure and Oxidation Behavior of Si–MoSi2 Functionally Graded Coating on Mo Substrate. – Ceramics International 43(8): 6250-6256.
[32] Zhang, Y., Ni, W., Li, Y. (2018): Effect of siliconizing temperature on microstructure and phase constitution of Mo–MoSi2 functionally graded materials. – Ceramics International 44(10): 11166-11171.
[33] Zhao, Q. M., Cheng, L., Liu, Z. T., Zhao, J. J. (2014): Surface characteristics of Zinc-TiO_2 coatings prepared via micro-arc oxidation. – Composite Interfaces 21(6): 585-593.
[34] Zhu, R. F., Wang, Z. G., Xiao, G. Y., Li, S., Lu, Y., Hanawa, T., Kobayashi, M. (2008): Effect of electrode voltage on microstructure and performance of micro-arc oxidized ceramic film on surface of pure titanium. – Journal of the chinese ceramic society 36(5): 631-635.

http://www.aloki.hu ● ISSN 1589 1623 (Print) ● ISSN 1785 0037 (Online)
DOI: http://dx.doi.org/10.15666/aeer/1704_86318641